Microchimica Acta (2020) 187:321
https://doi.org/10.1007/s00604-020-04299-3

ORIGINAL PAPER

Synergy between nanozymes and natural enzymes on the hybrid MoS_2 nanosheets/graphite microfiber for enhanced voltammetric determination of hydrogen peroxide

Jian Zhang[1,2] · Dong Han[3] · Yanhui Wang[2] · Longwei Wang[1] · Xuanyu Chen[1] · Xiran Qiao[4] · Xin Yu[1]

Received: 10 January 2020 / Accepted: 23 April 2020

Abstract

A biosensor for hydrogen peroxide (H_2O_2) has been developed based on the use of MoS_2 nanosheets and graphite that are assembled to form a microfiber hybrid structure. The MoS_2 nanosheets are synthesized in situ on a graphite microfiber. The chemical composition and surface morphology of the microfiber hybrid structure has been characterized. The microfiber is shown to display peroxidase-mimicking activity. In the next step, horseradish peroxidase, methylene blue, and chitosan are co-immobilized on the microfiber electrode. The use of MoS_2 nanosheets warrants high electrochemical activity of immobilized enzyme on the electrode surface. The modified microfiber electrode, best operated at a voltage of − 0.3 V (vs. Ag/AgCl), can be used to sense H_2O_2 with a linear response in the 0.1 to 90 μM concentration range and with a determination limit of 30 nM (at $S/N = 3$). The good response is attributed to the synergistic enhancement of the synthetic nanozymes (few-layered MoS_2 nanosheets) and immobilized natural horseradish peroxidase (HRP).

Keywords MoS_2 nanosheets/graphite microfiber · H_2O_2 determination · Electrochemical sensor · Peroxidase-like activity

Introduction

The accurate determination of hydrogen peroxide (H_2O_2) plays an important role in many areas including industrial production, clinical control, and environmental conservation [1]. According to the US Food and Drug Administration, the residual amount of H_2O_2 in food should not exceed 0.5 ppm [2]. In living organisms, H_2O_2 also plays an important role as a signaling molecule in a variety of biological regulation processes, such as immune cell activation, vascular remodeling, apoptosis, and stomatal closure [3]. It is necessary to determine H_2O_2, as low as possible. Electrochemistry is considered as a convenient method for H_2O_2 determination, because it has good sensitivity, time efficiency, and low cost [4, 5]. Horseradish peroxidase (HRP) is the most common enzyme for H_2O_2 sensing based on the electrochemical method [6–8]. Electrochemical communication from the electrode surface to the redox active center of enzymes is very eventful for the enzyme-based biosensors. Unfortunately, the redox active center is normally located deep in the thick protein shell. For most redox enzymes, direct electron transfer is a very inefficient process. Much effort has been focused on facilitating the electron transfer between proteins and electrodes. Electron transfer mediators such as toluidine blue, thionine, and methylene blue (MB) are typically used, which can minimize the effects of interferences and lower the operating potential of the electrodes [9, 10]. Efficient immobilization of redox enzyme and electron mediator should be adopted to enhance the performance of the biosensor. Nanomaterials or nanostructured electrodes have been developed in many enzyme-based biosensors. For example, metal nanoparticles [1], metal oxide nanostructures [11], or carbon nanomaterials [12, 13] can provide a favorable surface for the

Electronic supplementary material The online version of this article (https://doi.org/10.1007/s00604-020-04299-3) contains supplementary material, which is available to authorized users.

✉ Xin Yu
ifc_yux@ujn.edu.cn

[1] Institute for Advanced Interdisciplinary Research (iAIR), University of Jinan, Jinan 250022, People's Republic of China

[2] Institut Charles Gerhardt de Montpellier, UMR 5253, Université de Montpellier, CNRS, ENSCM, 34095 Montpellier Cedex 5, France

[3] Université de Lyon, Ecole Centrale de Lyon, UMR CNRS 5270, Institut des Nanotechnologies de Lyon, UMR CNRS 5270, 69130 Ecully, France

[4] School of Textile Science and Engineering, Tiangong University, Tianjin 300387, People's Republic of China

Published online: 12 May 2020

immobilization of enzymes allowing them to retain their biological activity due to the enhanced orientation freedom and good biocompatibility. Because of the physical and chemical properties, two-dimensional (2D) metal dichalcogenides nanomaterials have caused a lot of attention in the past few years, finding use in catalysis, batteries, and biosensors [14, 15]. For example, molybdenum disulfide (MoS_2) prepared by exfoliated from bulk or fabricated through hydrothermal methods have been used in enzyme-based biosensors [16, 17]. In addition, few-layer MoS_2 nanosheets with high surface area exhibited high adsorption capacity for MB. It has been reported that MB immobilized on MoS_2 can avoid leach during the testing [18]. Xiang et al. prepared a trimetallis hybrid nanoflower-decorated MoS_2 nanosheet for enhanced catalytic electrochemical reduction of H_2O_2 [19].

Furthermore, artificial enzyme mimics, especially nanozymes, are widely studied for H_2O_2 determination based on colorimetric methods [20]. MoS_2, also known as nanozymes, have activities similar to natural enzymes [21]. MoS_2 nanosheets have an intrinsic peroxidase-like catalytic activity. MoS_2 nanosheets have been shown to catalyze the oxidation of 3,3′,5,5′-tetramethylbenzidine (TMB) in the presence of H_2O_2 to result in a blue-colored oxidized product [22]. Zhang synthesized a *N*-doped carbon nanotubes@MoS_2 hybrid composites with enhanced peroxidase-like mimics to colorimetrically detect H_2O_2 [23].

Graphite microfiber electrodes have attracted much more interest than other solid electrodes (glass carbon or gold electrode). They have unique one-dimensional morphology and high electronic conductivity. Compared to the commonly used solid electrodes, instead of physical adsorption or chemical assembly of nanomaterials on electrode surface, different nanostructures can be in situ synthesized on the microfiber surface. It leads to a larger specific surface areas, high utilization efficiency, and excellent electron transfer process. In addition, flexible fiber electrodes have smaller sizes and can potentially be used in vivo. Several fibrous biosensors based on hybrid nanostructures were studied for biomolecule determination [24–27].

In this paper, in situ few-layered MoS_2 nanosheets-on-graphite fibers were constructed via a hydrothermal method. Three-dimensional MoS_2 nanosheets/graphite microfiber were obtained. A high-performance fibroid H_2O_2 electrochemical biosensor was fabricated by assembling HRP, chitosan, and methylene blue (MB) molecules on the MoS_2 nanosheets/graphite microfiber surface. For the first time, the action of nanozymes (few-layered MoS_2 nanosheets) and natural enzymes (immobilized HRP) was combined to study the highly sensitive electrochemical determination of H_2O_2. This hybrid structure became a favorable H_2O_2 determination biosensor with high sensitivity. The hybrid MoS_2 nanosheets/graphite microfiber electrodes might have the potential to detect different biomolecules, which would become an outstanding platform for in vitro or vivo determination.

Experimental

Materials

Horseradish peroxidase (HRP), methylene blue (MB), and chitosan were obtained from Sigma (https://www.sigmaaldrich.com/). A 30% hydrogen peroxide (H_2O_2) solution and 3, 3′,5,5′-tetramethyl-bezidine (TMB) were purchased from Beijing Chemical Reagent (http://www.gbw114.com/index.html), and H_2O_2 solutions were freshly prepared before use. Phosphate buffer (0.1 M) with various pH values was prepared by Na_2HPO_4 and NaH_2PO_4. Graphite microfibers were obtained from Toray (M40-JB-12 K) (Japan) (https://www.toray.cn/products/prod_004.html). All the reagents used in this work are of analytic grade and are commercially available.

Fabrication of MoS_2 nanosheets/graphite microfiber and enzyme immobilization

Graphite fibers were washed in 3.0 M HNO_3, 1.0 M KOH, and distilled water sequentially by ultrasonic cleaning for several minutes before synthesis [28]. MoS_2 nanosheets were synthesized on graphite fibers through a typical hydrothermal method [29]. Graphite fibers (about 4 cm long) were put into a 25-mL autoclave, containing the solution of mixing sodium molybdate dehydrate ($Na_2MoO_4{\cdot}2H_2O$) (60 mg), thioacetamide (C_2H_5NS) (30 mg), and distilled water (20 mL). The autoclave was heated at 200 °C for 24 h. After cooling down to the room temperature, the microfibers were then placed out and then washed by the ultrapure water, followed by drying at 50 °C in the vacuum. Five milligrams of HRP and MB was dispersed and mixed in 2 mL 0.3 wt% chitosan under stirring for 30 min. Chitosan is a natural polymer product and its biodegradability, non-toxicity, and biocompatibility make it a promising matrix for enzyme immobilization. Chitosan can be dissolved in weak acid and can be easily formed an organic film on the solid electrodes, which is widely used in biosensors. After that, MoS_2 nanosheets/graphite microfibers were immersed in the HRP/MB/chitosan mixture solution for 60 min, followed by drying at 4 °C overnight. At last, the HRP/MB/chitosan/MoS_2/graphite microfiber was obtained. MB/chitosan/MoS_2/graphite microfiber was prepared with the similar method without HRP adding.

Surface characterization and electrochemical measurements

The morphologies and surface structures were characterized with field-emission scanning electron microscope (SEM, HITACHI S8020, Japan) and transmission electron

microscopy (TEM, JEM 2100F, Japan). Raman spectroscopy was measured at the excitation line of 532 nm (LabRAM HR Evolution, HORIBA). X-ray diffraction (XRD) patterns were collected with a D8 ADVANCE diffractometer with Cu Kα radiation (λ = 1.5406 Å). X-ray photoelectron spectroscopy (XPS) was performed using an ESCALAB 250 photoelectron spectrometer (Thermo Fisher Scientific) with a monochromatic Al Kα X-ray beam (1486.60 eV).

The electrochemical experiment was carried out in a three-electrode system. Ag/AgCl (saturated KCl) (32 mm (long) × 1.5 mm (diameter) straight line) electrode was used as the reference electrode. Pt plate electrode (1 cm × 1 cm) was used as the counter electrode. HRP/MB/chitosan/MoS_2/graphite microfiber electrode (10 mm in length) was used as the working electrode. All the measurements were performed using a Gamry electrochemical workstation (Reference 3000, America).

Peroxidase-like catalytic activity of MoS_2

The color change of peroxidase-like few-layered MoS_2 towards TMB was photographed at room temperature after 5 min of co-incubation. The few-layered MoS_2 used is scraped from the graphite microfiber. The steady-state kinetic assay of the MoS_2 to TMB in the presence of H_2O_2 was carried out at room temperature. TMB and hydrogen peroxide are dispersed into deionized water. The final concentrations of TMB and H_2O_2 were 1 mM and 10 mM. Then, add different amounts of MoS_2 to a final concentration of 0, 50, 100, 150, and 200 μg mL^{-1}, respectively. Then, UV–vis spectra measurements in a quartz cuvette with an optical path length of 1 cm.

Results and discussion

The composition and phase structure of the MoS_2 nanosheets/graphite microfiber were first investigated by XRD and Raman. As shown in Fig. 1a, the diffraction peak of the graphite microfiber (curve b) centered at $2\theta = 25.7^{o}$ can be referenced as graphite (JCPDS no. 65–6212). On curve c of MoS_2 nanosheets/graphite microfiber besides the graphite peaks, the other peaks are contributed to the diffraction peaks of MoS_2 (JCPDS no. 37–1492, curve a) [29]. Further, Raman spectra (Fig. 1b) was performed on this hybrid fiber to demonstrate the existence of MoS_2. As shown in curve a, typical G peaks and D peaks are clearly observed at around 1585 cm^{-1} and 1350 cm^{-1}, respectively. Compared with the graphite fiber, the Raman spectrum shows typical features of MoS_2: the E^1_{2g} peaks at 385 cm^{-1} and A_{1g} peaks at 408 cm^{-1} (curve b) [30].

SEM and TEM analysis was carried out to study the surface morphology of the MoS_2 nanosheets/graphite microfiber. Commercial graphite fibers have a diameter of approximately 5 μm and a smooth surface (Fig. 1c). Figure 1 d shows that the graphite microfiber is densely buried by the layered MoS_2 nanosheets with uniform size after hydrothermal synthesis. MoS_2 nanosheets are randomly interconnected with each other to form a porous surface. By comparing Fig. 1 c and d, the thickness of MoS_2 is about 0.8 μm. Measuring from the curved edges of the nanosheets, the thickness of the MoS_2 nanosheets is determined to be about 5–8 nm (Fig. 1e). Fig. S1 shows more SEM images about the MoS_2 nanosheets/graphite microfiber hybrid nanostructures. TEM images show that the vertical edges of MoS_2 nanosheets exfoliated from the hybrid microfibers' surface has a layered structure (Fig. 1f). In addition, from the inset of Fig. 1f, it clearly reveals a layered structure with a layer-to-layer distance of 0.65 nm, which corresponds to the (002) planes of MoS_2 crystals [31]. The MoS_2 nanosheet was about 10 layers. The above results demonstrate that MoS_2 nanosheets/graphite microfiber hybrid electrodes have been successfully fabricated. The chemical composition and valence state of the MoS_2 nanosheets were characterized by X-ray photoelectron spectroscopy (XPS), as shown in Fig. S2. The binding energies (BEs) of 231.09 and 228.8 eV are Mo $3d_{3/2}$ and Mo $3d_{5/2}$, respectively, ascribed to the Mo^{4+} oxidation state (Fig. S2A). The BE of 163.2 eV in Fig. S2B corresponds to the S 2p [32].

The catalytic performances of the MoS_2 nanosheets/graphite microfiber were evaluated for catalyzing the reaction of peroxidase substrate 3, 3′, 5, 5′-tetramethyl-bezidine (TMB) with H_2O_2. The MoS_2 can catalyze oxidation of TMB in the presence of H_2O_2 (10 mM), and a blue color was observed after reaction of 5 min (Fig. 2a). It is clearly observed that the absorbance at 368 and 652 nm increases gradually, which indicates the formation of blue one-electron oxidation product, TMB^+. As no catalysts are added, there are no color changes in the solution and the absorbance at 652 nm is closed to zero, indicating that the reaction of the oxidation of TMB by H_2O_2 almost ceased. Furthermore, the catalytic activity was proved to be dependent on the concentrations of MoS_2 (Fig. 2b). The large surface area of three-dimensional MoS_2 nanosheets/graphite microfiber may provide more catalytic sites for the reaction of TMB with H_2O_2, thus exhibiting high enzymatic peroxidase ability.

After HRP immobilization, the electrochemical characterization of graphite microfiber, MoS_2/graphite microfiber HRP/chitosan/MoS_2/graphite microfiber (without MB) was carried out using the electrochemical impedance spectra (EIS). The charge transfer process is found to be influenced by the different surface modification. Figure 3 a shows the typical EIS Nyquist plots obtained from three electrodes in the $K_3[Fe(CN)_6]/K_4[Fe(CN)_6]$ mixture. The charge transfer resistance (R_{ct}) of the MoS_2/graphite microfiber is smaller than that of the graphite microfiber, demonstrating that the electron transfer rate increases on the MoS_2/graphite microfiber with the presence of MoS_2 nanosheets. MoS_2 nanosheets increase

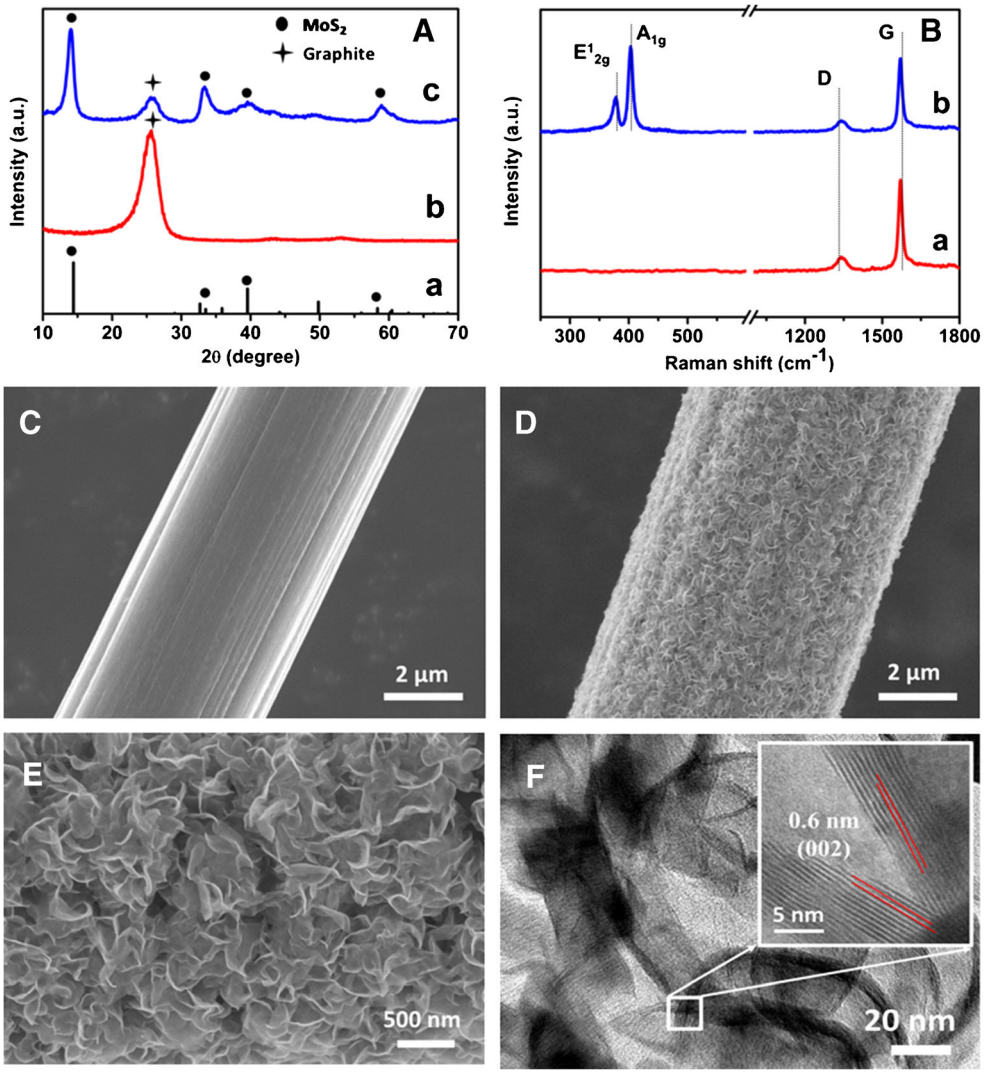

Fig. 1 **a** XRD patterns of a MoS_2 (JCPDS no. 37–1492), b graphite microfiber, and c MoS_2 nanosheets/graphite microfiber. **b** Raman spectra of a graphite microfiber and b MoS_2 nanosheets/graphite microfiber. SEM images of **c** graphite microfiber, **d** MoS_2 nanosheets/ graphite microfiber, and **e** MoS_2 nanosheets. **f** TEM image of MoS_2 nanosheets. The inset is a high resolution TEM image of the region within the white rectangle

the microfiber electrode surface area, and two-dimensional layered structures contribute to the electron transfer process. However, R_{ct} increased (curve c) after the HRP was immobilized on the MoS_2 nanosheets/graphite microfiber electrode surface, indicating that these chemical compounds film was formed on the MoS_2 nanosheets/graphite microfiber electrode surface and blocked the electron transfer between the $K_3[Fe(CN)_6]/K_4[Fe(CN)_6]$ probe and electrode surface [33]. The impedance spectrum is interpreted by fitting with an equivalent circuit (Fig. S3). In this circuit, Rs represents the resistance of the solution, Rct represents the resistance to charge transfer between the solution and the electrode surface, W is the Warburg impedance due to the contribution of diffusion, and CPE is associated with the capacitance of the double

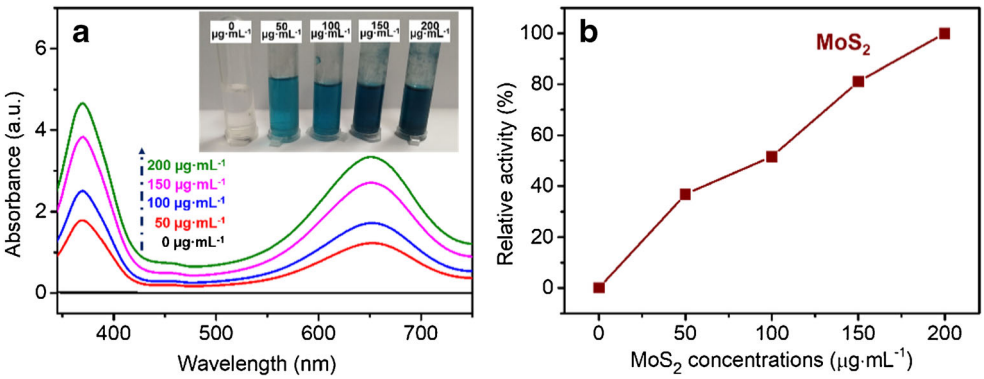

Fig. 2 **a** UV–vis spectra of MoS_2 + TMB (1 mM) + H_2O_2 (10 mM) with different concentration of MoS_2. Inset shown the photographs of the reaction system. **b** MoS_2 concentration-dependent peroxidase-activity with TMB (1 mM) and H_2O_2 (10 mM)

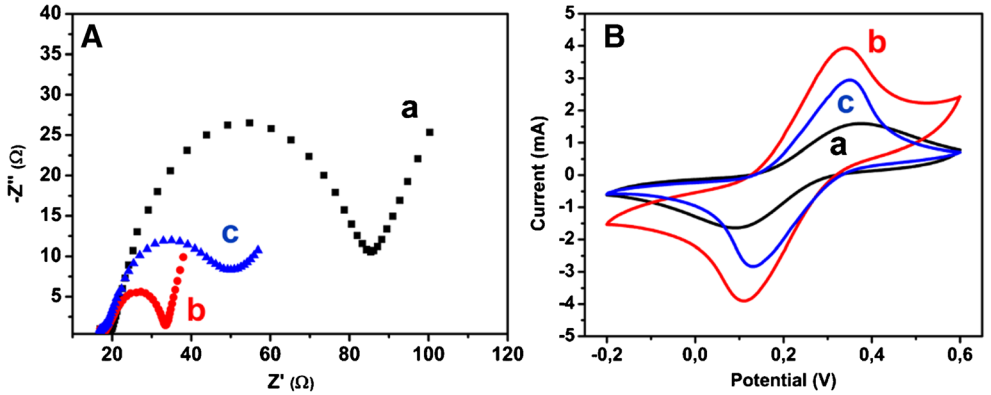

Fig. 3 **a** EIS Nyquist plot of (a) graphite microfiber electrode, (b) MoS_2/graphite microfiber electrode, and (c) HRP/chitosan/MoS_2/graphite microfiber electrodes. **b** CV curve of (a) graphite microfiber electrode, (b) MoS_2/graphite microfiber electrode, and (c) HRP/chitosan/MoS_2/graphite microfiber electrodes. **a** and **b** were both recorded in 0.01 M phosphate buffer containing 5 mM $K_3[Fe(CN)_6]/K_4[Fe(CN)_6]$ and 0.1 M KCl (pH 7.4)

layer. The simulated values of the equivalent circuit elements after every modified step are summarized in Table S1. Cyclic voltammetry curves with the same electrodes were also recorded to explore the electrochemistry behavior, and the results are similar to those found with the EIS (Fig. 3b). The peak current increases after the introduction of MoS_2 nanosheets. The electro-active surface area of electrode can be estimated for a reversible and diffusion-controllable process according to the Randles–Sevcik equation [34]:

$$I_p = 2.69 \times 10^5 A D^{1/2} n^{3/2} r^{1/2} C$$

where A is the geometrical surface area, D is the diffusion coefficient ($6.7 \pm 0.02 \times 10^{-6}$ cm^2 s^{-1}), n is the number of electrons, r is the scan rate (V s^{-1}), and C is the concentration (mol cm^{-3}). The calculated geometrical surface area of the graphite microfiber electrode and MoS_2/graphite microfiber electrode is 1.2 and 6.0 cm^2. An increase in the surface area in the MoS_2/graphite microfiber electrode is attributed to the increased surface area of the nanosheets. However, the peak current decreases after the immobilization of enzyme, indicating a weakened electron transfer process compared to that of the MoS_2 nanosheets/graphite microfiber electrode. The result suggests the successful assembly of enzyme film on the MoS_2 nanosheets/graphite microfiber electrode surface. The peak current of HRP/chitosan/MoS_2/graphite microfiber decreased compared to that of the MoS_2/graphite microfiber electrode. Indeed, the rate of electron transfer is dependent of the thickness of the organic layer formed on electrodes. The thicker the organic layer, the slower the rate of electron transfer. Here, a passivated organic layer formed after the immobilization of enzyme biomolecules, resulting in a weakened electron transfer process. These results suggest successful assembly of HRP film on the MoS_2 nanosheets/graphite microfiber electrode surface. The SEM images of MOS_2/graphite fiber after HRP immobilization is shown in Fig. S4.

The cyclic voltammetry is chosen to investigate the changes of electrode behavior after each assembly step. From the curve a, b, c and d in Fig. 4a, there are no redox peaks. The background current of the MoS_2/graphite microfiber (curve b) is higher than that of the graphite microfiber, which is attributed to the large surface area of the MoS_2 nanosheets. However, at the HRP/MB/chitosan/MoS_2/graphite microfiber, one pair of well-defined redox peaks is observed (curve e), suggesting the successful assembly of MB on the designed electrode. To investigate the influence of MoS_2 nanosheets on graphite microfiber, we had tested the cyclic voltammograms (Fig. 4b). It is clear that the peak current of HRP/MB/chitosan/MoS_2/graphite microfiber (curve b) is obviously higher than HRP/MB/chitosan/graphite microfiber (curve a). Signal enhancement may be attributed to facilitation of electron transfer reaction between the graphite fiber and MB by localization of MoS_2 nanosheets. It may also be due to extension of the surface area due to immobilization of MoS_2 nanosheets on the fiber surface.

To better understand the electrochemistry of the HRP/MB/chitosan/MoS_2/graphite microfiber electrodes, further CV measurements were carried out at different scan rates. Figure 5 a shows the cyclic voltammograms of the HRP/MB/chitosan/MoS_2/graphite microfiber electrodes in 0.1 M phosphate buffer (pH 7.0) at different scan rates from 80 to 200 mV s^{-1}. There is no obvious potential shift on both cathodic and anodic peak with the increasing scan rates. The anodic current and cathodic peak current increase linearly with the increasing scan rates, revealing that the redox reaction on the HRP/MB/chitosan/MoS_2/graphite microfiber electrodes is a quasi-reversible diffusion-controlled electrochemical process (Fig. 5b) [5].

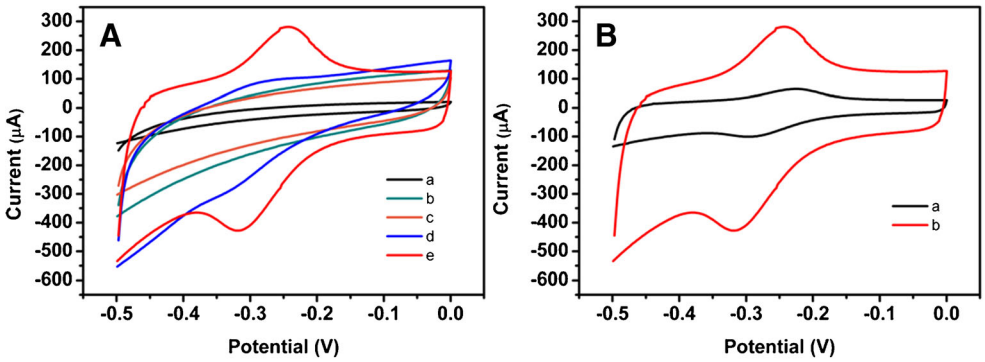

Fig. 4 **a** The cyclic voltammograms of graphite microfiber (a), MoS_2/graphite microfiber (b), chitosan/MoS_2/graphite microfiber (c), HRP/chitosan/MoS_2/graphite microfiber (d), and HRP/MB/chitosan/MoS_2/graphite microfiber (e) in 0.1 M N_2-saturated phosphate buffer at a scan rate of 100 mV s^{-1} (pH 7.0). **b** Cyclic voltammograms of HRP/MB/chitosan/graphite microfiber (a) and HRP/MB/chitosan/MoS_2/graphite microfiber (b) in 0.1 M N_2-saturated phosphate buffer at a scan rate of 100 mV s^{-1} (pH 7.0)

The electrochemical properties of MB/chitosan/MoS_2/graphite microfiber electrodes before and after natural enzyme HRP immobilization towards the reduction of H_2O_2 were studied by CV method. As shown in Fig. 6, it displays the typical CV curves of two electrodes recorded in 0.1 M phosphate buffer (pH 7.0) in the absence (curve a, b) and in the presence of 2×10^{-4} M H_2O_2 (curve c, d). Firstly, the electrocatalytic activity of MB/chitosan/MoS_2/graphite microfiber without HRP immobilization towards reduction of H_2O_2 is evaluated. In the absence of H_2O_2, it shows a defined redox peak based on the introduction of mediator MB on the microfiber electrode surface (curve a). After the addition of H_2O_2 (curve c), the reduction current increased greatly compared with curve a, indicating obvious catalytic reduction of MB/chitosan/MoS_2/graphite microfiber electrodes towards H_2O_2. However, there is no obvious current difference of MB/chitosan/graphite microfiber towards the reduction of H_2O_2 (Fig. S5), which indicates that the MoS_2 nanosheets exhibited good enzymatic activity. Secondly, the electrocatalytic activity of HRP/MB/chitosan/MoS_2/graphite microfiber electrodes towards reduction of H_2O_2 is evaluated. In the absence of H_2O_2, the curve shows a well-defined redox peak (curve b). The reduction current of the HRP/MB/chitosan/MoS_2/graphite microfiber is significantly increased in the presence of H_2O_2 (curve d). The increase of reduction current of HRP/MB/chitosan/MoS_2/ graphite microfiber before and after H_2O_2 adding is higher than the one of MB/chitosan/MoS_2/graphite microfiber, which results from the additional HRP immobilization. H_2O_2 added to the solution is first reduced by HRP (red), by which HRP (ox) is formed. Secondly, the HRP (red) is regenerated by the mediator MB molecule, so that the MB (red) is oxidized to become MB (ox). Finally, the MB (ox) is reduced on the electrode surface. In this way, MB as an electron mediator accelerates the electron transfer. As the previous study, few-layered MoS_2 nanosheets, as a nanozyme, displayed considerable catalytic performance towards reduction of H_2O_2. 3D MoS_2 nanosheet hybrid structure is constructed here, which provide large specific surface area for enhancing the natural enzyme HRP immobilization. Few-layered MoS_2 nanosheets are directly connected to graphite fiber surface for an enhanced electron transport. As a result, the HRP/MB/chitosan/MoS_2/graphite microfiber has enhanced electrocatalytic activity towards reduction of H_2O_2. HRP/MB/chitosan/MoS_2/graphite microfiber can have a good catalytic response to H_2O_2 through synergistic enhancement of nanozymes (few-layered MoS_2 nanosheets) and natural enzymes (immobilized HRP). The scheme of nanozymes

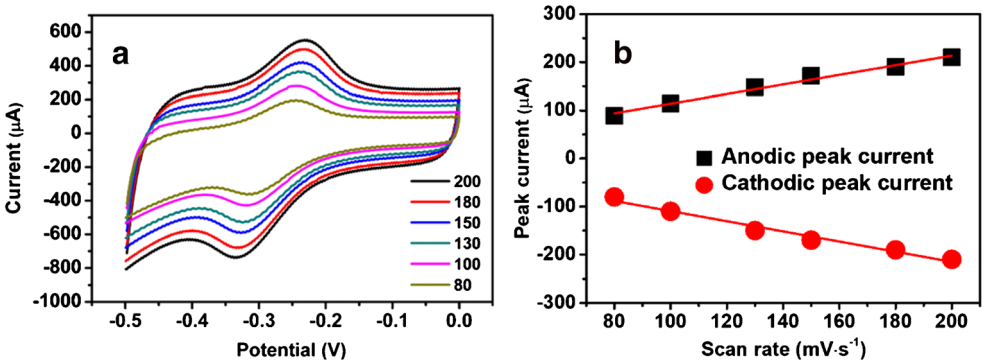

Fig. 5 **a** CV of HRP/MB/chitosan/MoS_2/graphite microfiber electrodes in 0.1 M N_2-saturated phosphate buffer (pH 7.0) at different scan rate from 80 to 200 mV s^{-1} (from inside to outside). **b** Anodic and cathodic peak currents plotted against scan rate

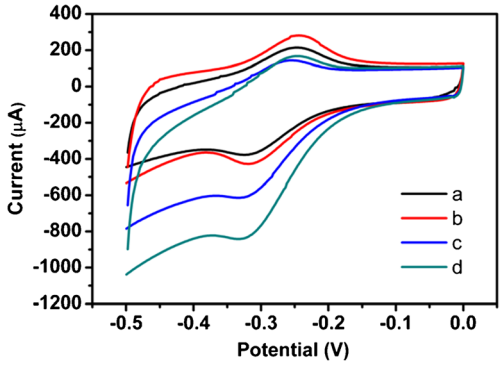

Fig. 6 The cyclic voltammograms of MB/chitosan/MoS_2/graphite microfiber in the absence (**a**) and presence (**c**) of 2×10^{-4} M H_2O_2 in 0.1 M phosphate buffer at a scan rate of 100 mV s^{-1} (pH 7.0). The cyclic voltammograms of HRP/MB/chitosan/MoS_2/graphite microfiber in the absence (**b**) and presence (**d**) of 2×10^{-4} M H_2O_2 in 0.1 M phosphate buffer at a scan rate of 100 mV·s^{-1} (pH 7.0)

and natural enzymes synergy enhanced H_2O_2 response based on few-layered MoS_2 nanosheets/graphite microfibers filament structure is shown in Scheme 1.

The amperometric response of the HRP/MB/chitosan/MoS_2/graphite microfiber electrodes was tested. The applied potential and pH value were optimized state (Fig. S6, S7). Figure 7 a shows the typical current response plots of different microfiber electrodes in successive injections of 8 μM H_2O_2 into the 0.1 M phosphate buffer (pH 7.0) under the optimized operating electrode potential of − 0.3 V. The amperometric response of the HRP/MB/chitosan/MoS_2/graphite microfiber (curve d) to H_2O_2 is higher than that of HRP/MB/ chitosan/graphite microfiber (b) and MB/chitosan/MoS_2/graphite microfiber (c). The results show that nanoenzyme MoS_2 nanosheets enhance and contribute to the electrochemical activity of HRP towards H_2O_2. Nanozymes (MoS_2 nanosheets) and natural enzymes (immobilized HRP) synergy enhanced H_2O_2 determination is proposed. Figure 7 b shows the calibrations of three electrodes towards to H_2O_2 from the current response shown in Fig. 7a. The HRP/MB/chitosan/MoS_2/graphite microfiber electrodes have the best H_2O_2 response among these three electrodes. The HRP/MB/chitosan/MoS_2/graphite microfiber electrode shows a linear response to H_2O_2 concentrations within the range of 1×10^{-7}–9×10^{-5} M (correlation coefficient 0.996) with a determination limit of 3×10^{-8} M (based on S/N = 3). The repeatability of the biosensor was investigated by amperometric measurements. The sensor exhibits acceptable repeatability of 3.3% for 10 successive measurements.

The HRP/MB/chitosan/MoS_2/graphite microfiber biosensor exhibits high selectivity for H_2O_2 determination. As shown in Fig. 7c, HRP/MB/chitosan/MoS_2/graphite microfiber electrodes showed obvious amperometric response towards 0.2 mM H_2O_2. With a further injection of 1 mM ascorbic acid (AA), uric acid (UA), dopamine (DA), or 1 mM inorganic ions (Na^+, K^+, Mg^{2+}, Ca^{2+}, and Cl^-), there were no noteworthy amperometric responses observed. The microfiber electrode retains 89% of its initial current response after 60 days (Fig. 7d), which was stored in the phosphate buffer (pH 7.0) at 4 °C when unused, which demonstrates the hybrid fiber electrode is stable for a long time to retain an acceptable detection performance. In addition, six HRP/MB/chitosan/MoS_2/graphite microfiber electrodes were prepared in the same way to evaluate the precision of the proposed strategy, and a RSD of 3.6% was achieved, indicating the high reproducibility reliability of the method.

Conclusions

In summary, few-layered MoS_2 nanosheets have been prepared on graphite microfiber surface to form hybrid

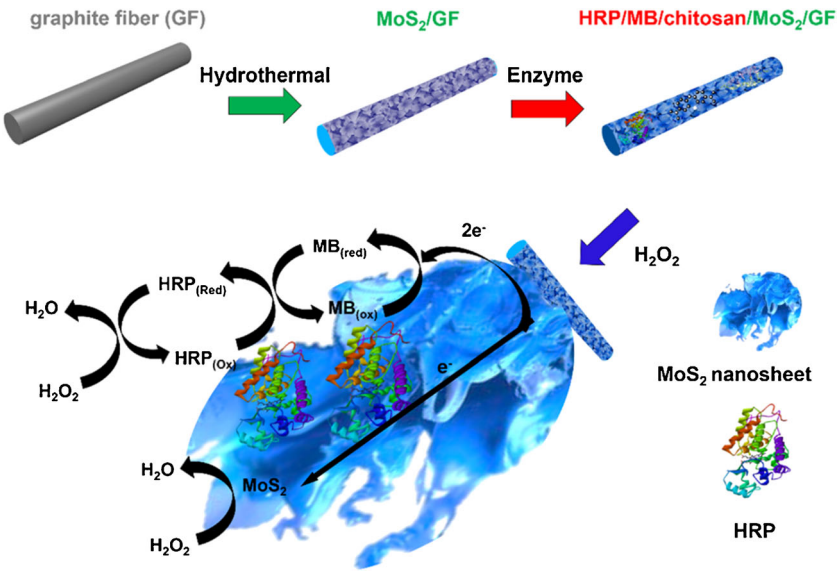

Scheme 1 Nanozymes and natural enzymes synergy enhanced H_2O_2 response on few-layered MoS_2 nanosheets/graphite microfibers filament structure.

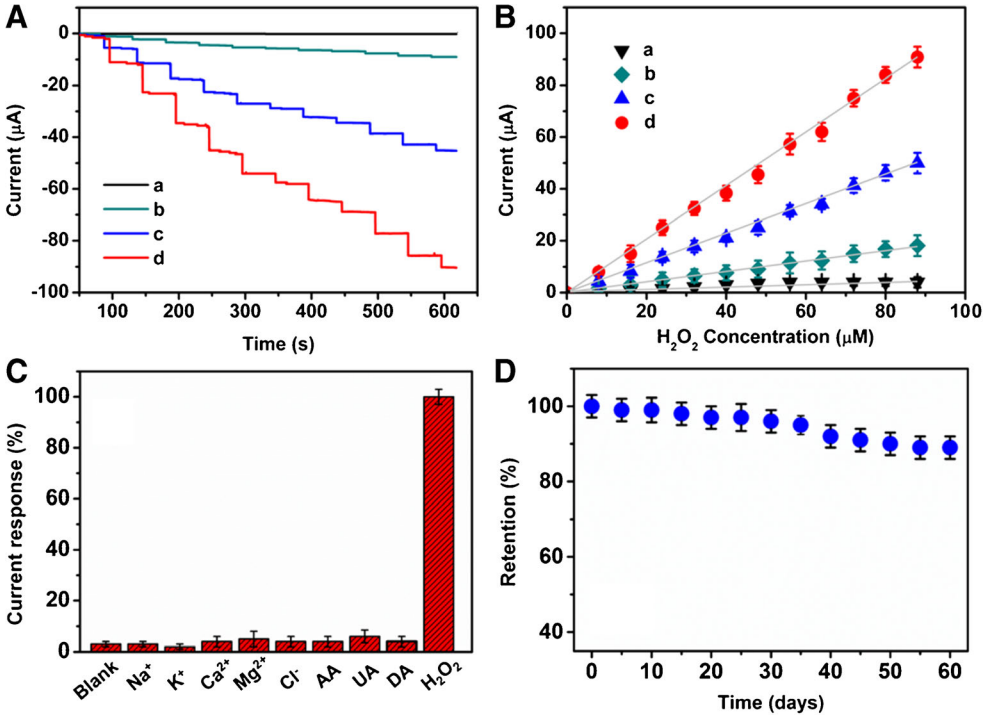

Fig. 7 **a** Amperometric response of graphite microfiber (a), HRP/MB/chitosan/ graphite microfiber (b), MB/chitosan/MoS_2/graphite microfiber (c), and HRP/MB/ chitosan/MoS_2/graphite microfiber (d) with total additions of 8.8×10^{-5} M H_2O_2 in 0.1 M phosphate buffer (pH 7.0) at the operating potential of − 0.3 V. **b** Graphite microfiber (a), HRP/MB/chitosan/graphite microfiber (b), MB/chitosan/MoS_2/graphite microfiber (c), and HRP/MB/chitosan/MoS_2/graphite microfiber (d). **c** Amperometric response of HRP/MB/chitosan/MoS_2/graphite microfiber electrodes to various interferences. The response current of HRP/MB/chitosan/MoS_2/graphite microfiber electrodes towards 0.2 mM H_2O_2 is set as 100%, and the response currents towards 1 mM AA, UA, DA, Na^+, K^+, Mg^{2+}, Ca^{2+}, and Cl^- are normalized to this value. **d** Stability of HRP/MB/chitosan/MoS_2/graphite microfiber electrodes. (The error bars represent one standard deviation from the mean, $n = 3$)

MoS_2 nanosheets/graphite microfiber. It proves that the MoS_2 nanosheet/graphite microfiber has peroxidase mimicking activity towards H_2O_2 by colorimetric method. In addition, MoS_2 nanosheets provide many sites for natural enzyme HRP immobilization. The action of nanozymes and natural enzymes performed highly sensitive electrochemical determination of H_2O_2. The biosensor based on hybrid MoS_2 nanosheets/graphite microfiber behaves excellent sensitivity and selectivity, high stability, excellent practicality along with appropriate reproducibility. Due to the fiber morphology and flexibility of 3D electrodes, H_2O_2 can be monitored in certain harsh environments, even in target cells or in vivo. Furthermore, we propose that MoS_2 nanosheet/graphite microfiber will become an important platform for building different types of highly sensitive and selective biosensors, thereby opening broad opportunities for biotechnology.

Acknowledgments The work was supported by the National Natural Science Foundation of China (No. 51802115), the Natural Science Foundation of Shandong Province (No. ZR2018BEM010, No. ZR2019YQ21), the Major Program of Shandong Province Natural Science Foundation (No. ZR2018ZC0843), and the Scientific and Technology Project of University of Jinan (No. XKY1923).

Compliance with ethical standards

Conflict of interest The authors declare that they have no conflict of interest.

References

1. Wang L, Wang ER (2004) A novel hydrogen peroxide sensor based on horseradish peroxidase immobilized on colloidal Au modified ITO electrode. Electrochem Commun 6:225–229. https://doi.org/10.1016/j.elecom.2003.12.004
2. Ito A, Sato Y, Kudo S, Sato S, Nakajima H, Toba T (2003) The screening of hydrogen peroxide-producing lactic acid Bacteria and their application to inactivating psychrotrophic food-borne pathogens. Curr Microbiol 47:0231–0236. https://doi.org/10.1007/s00284-002-3993-1
3. Veal EA, Day AM, Morgan BA (2007) Hydrogen peroxide sensing and signaling. Mol Cell 26:1–14. https://doi.org/10.1016/j.molcel.2007.03.016
4. Lacina K, Kubesa O, Vanysek P, Horackova V, Moravec Z, Skladal P (2017) Selective electrocatalysis of reduced graphene oxide towards hydrogen peroxide aiming oxidases-based

biosensing: caution while interpreting. Electrochim Acta 223:1–7. https://doi.org/10.1016/j.electacta.2016.11.172

5. Kafi AKM, Wu GS, Benvenuto P, Chen AC (2011) Highly sensitive amperometric H_2O_2 biosensor based on hemoglobin modified TiO_2 nanotubes. J Electroanal Chem 662:64–69. https://doi.org/10.1016/j.jelechem.2011.03.021
6. Wang F, Gong W, Wang L, Chen Z (2015) Enhanced amperometric response of a glucose oxidase and horseradish peroxidase based bienzyme glucose biosensor modified with a film of polymerized toluidine blue containing reduced graphene oxide. Microchim Acta 182:1949–1956. https://doi.org/10.1007/s00604-015-1535-3
7. Cheng X, Sun L, Li R, Huang Y, Xu H, Wang Z, Li Z, Jiang H, Ma J (2019) Organic polymer dot-based fluorometric determination of the activity of horseradish peroxidase and of the concentrations of glucose and the insecticidal protein toxin Cry1Ab/Ac. Microchim Acta 186. https://doi.org/10.1007/s00604-019-3831-9
8. Wu S, Huang X, Tang Y, Ma L, Liu Y, Sun J (2020) Temperature controllable electrochemical sensors based on horseradish peroxidase as electrocatalyst at heated Au disk electrode and its preliminary application for H_2O_2 detection. Analytic Chimica Acta 1096:44–52. https://doi.org/10.1016/j.aca.2019.10.052
9. Xu J, Zhu J, Wu Q, Hu Z, Chen H (2003) An amperometric biosensor based on the coimmobilization of horseradish peroxidase and methylene blue on a carbon nanotubes modified electrode. Electroanal. 15:219–224. https://doi.org/10.1002/elan.200390027
10. Ye J, Baldwin PR (1988) Catalytic reduction of myoglobin and hemoglobin at chemically modified electrodes containing methylene blue. Anal Chem 60:2473. https://doi.org/10.1021/ac00171a021
11. Dai H, Chen Y, Niu X, Pan C, Chen H, Chen X (2018) High-performance electrochemical biosensor for nonenzymatic H_2O_2 sensing based on Au@C-Co_3O_4 heterostructures. Biosens Bioelectron 118:36–43. https://doi.org/10.1016/j.bios.2018.07.022
12. Periasamy AP, Ho YH, Chen SM (2011) Multiwalled carbon nanotubes dispersed in carminic acid for the development of catalase based biosensor for selective amperometric determination of H_2O_2 and iodate. Biosens Bioelectron. 29:151–158. https://doi.org/10.1016/j.bios.2011.08.010
13. Zhong L, Gan S, Fu X, Li F, Han D, Guo L, Niu L (2013) Electrochemically controlle growth of silver nanocrystals on graphene thin film and applications for efficient nonenzymatic H_2O_2 biosensor. Electrochim Acta 89:222–228. https://doi.org/10.1016/j.electacta.2012.10.161
14. Chhowall M, Liu Z, Zhang H (2015) Two-dimensional transition metal dichalcogenide (TMD) nanosheets. Chem Soc Rev 44:2584–2586. https://doi.org/10.1039/C5CS90037A
15. Huang X, Zeng Z, Zhang H (2013) Metal dichalcogenide nanosheets: preparation, properties and applications. Chem Soc Rev 42:1934–1946. https://doi.org/10.1039/C2CS35387C
16. Su S, Sun H, Xu F, Yuwen L, Fan C, Wang L (2014) Direct electrochemistry of glucose oxidase and a biosensor for glucose based on a glass carbon electrode modified with MoS_2 nanosheets decorated with gold nanoparticles. Microchim Acta 181:13–14. https://doi.org/10.1007/s00604-014-1178-9
17. Song H, Ni Y, Kokot S (2014) Investigations of an electrochemical platform based on the layered MoS_2–graphene and horseradish peroxidase nanocomposite for direct electrochemistry and electrocatalysis. Biosens Bioelectron. 56:137–143. https://doi.org/10.1016/j.bios.2014.01.014
18. Zhang C, Li X, Lian C, Hu C, Duo S, Hu Q (2018) Few-layered MoS_2 synthesized by hydrothermal method with improved adsorption capacity for methylene blue than active carbon. J Nanosci Nanotechno 18:7948–7951. https://doi.org/10.1166/jnn.2018.16108
19. Dou B, Yang J, Yuan R, Xiang Y (2018) Trimetallic hybrid nanoflower-decorated MoS_2 nanosheet sensor for direct in situ monitoring of H_2O_2 secreted from live cancer cells. Anal Chem 90:5945–5950. https://doi.org/10.1021/acs.analchem.8b00894
20. Wu J, Wang X, Wang Q, Lou Z, Li S, Zhu Y, Wei H (2019) Nanomaterials with enzyme-like characteristics(nanozymes): next-generation artificialenzymes (II). Chem Soc Rev 48:1004–1076. https://doi.org/10.1039/C8CS00457A
21. Chen T, Zou H, Wu X, Liu C, Situ B, Zhang L, Yang G (2018) Nanozymatic antioxidant system based on MoS_2 nanosheets. ACS Appl Mater Interfaces 10:12453–12462. https://doi.org/10.1021/acsami.8b01245
22. Lin T, Zhong L, Guo L, Fu F, Chen G (2014) Seeing diabetes: visual detection of glucose basedon the intrinsic peroxidase-like activity of MoS_2 nanosheets. Nanoscale 6:11856–11862. https://doi.org/10.1039/C4NR03393K
23. Zheng J, Song S, Chen H, Xu J, Alharbi N, Hayat T, Zhang M (2019) Enhanced peroxidase-like activity of hierarchical MoS_2-decorated N-doped carbon nanotubes with synergetic effect for colorimetric detection of H_2O_2 and ascorbic acid. Chin Chem Lett. https://doi.org/10.1016/j.cclet.2019.09.037
24. Zhang J, Han D, Wang S, Zhang X, Yang R, Ji Y, Yu X (2019) Electrochemical detection of adenine and guanine using a three-demensional WS_2 nanosheet/graphite microfiber hybrid electrode. Electrochem Comm 99:75–80. https://doi.org/10.1016/j.elecom.2019.01.007
25. Zhang J, Han D, Yang R, Ji Y, Liu J, Yu X (2019) Electrochemical detection of DNA hybridization based on three-dimensional ZnO nanowires/graphite hybrid microfiber structure. Bioelectrochemistry 128:126–132. https://doi.org/10.1016/j.bioelechem.2019.04.003
26. Zhang J, Yu X, Guo W, Qiu J, Mou X, Li A, Liu H (2016) Construction of titanium dioxide nanorod/graphite microfiber hybrid electrodes for a high performance electrochemical glucose biosensor. Nanoscale 8:9382–9389. https://doi.org/10.1039/C6NR01360K
27. Zhang J, Li A, Yu X, Guo W, Zhao Z, Qiu J, Mou X, Claverie JP, Liu H (2015) Scaly graphene oxide/graphite fiber hybrid electrodes for DNA biosensors. Adv Mater Interfaces 2:1500072. https://doi.org/10.1002/admi.201500072
28. Zhang M, Liu K, Xiang L, Lin Y, Su L, Mao L (2007) Carbon nanotube-modified carbon fiber microelectrodes for in vivo voltammetric measurement of ascorbic acid in rat brain. Anal Chem 79:6559–6565. https://doi.org/10.1021/ac0705871
29. Zhang Y, He T, Liu G, Zu L, Yang J (2017) One-pot mass preparation of MoS_2/C aerogels for high-performance supercapacitors and lithium-ion batteries. Nanoscale 9:10059–10066. https://doi.org/10.1039/C7NR03187D
30. Li H, Zhang Q, Yap CCR, Tay BK, Edwin THT, Olivier A, Baillargeat D (2012) From bulk to monolayer MoS_2: evolution of raman scattering. Adv Funct Mater 22:1385–1390. https://doi.org/10.1002/adfm.201102111
31. Chen YX, Wu X, Huang KJ (2018) A sandwich-type electrochemical biosensing platform for microRNA-21 detection using carbon

sphere-MoS_2 and catalyzed hairpin assembly for signal amplification. Sensor Actuators B: Chem 270:179–186. https://doi.org/10.1016/j.snb.2018.05.031

32. Wu Y, Li H, Ji L, Ye Y, Chen J, Zhou H (2013) Preparation and properties of MoS_2/a-C films for space tribology. J Phys D Appl Phys 46. https://doi.org/10.1088/0022-3727/46/42/425301
33. Kang X, Wang J, Wu H, Aksay I, Liu J, Lin Y (2009) Glucose oxidase–graphene– chitosan modified electrode for direct electrochemistry and glucose sensing. Biosens Bioelectron. 25:901–905. https://doi.org/10.1016/j.bios.2009.09.004
34. Wang A, Silva TA, Filho O (2017) Graphite oxide and gold nanoparticles as alternative materials in the design of a highly sensitive electrochemical sensor for the simultaneous determination of biological species. Electroanal. 29:2491–2497. https://doi.org/10.1002/elan.201700357